GW190521: A Binary Black Hole Merger with a Total Mass of 150 $M_{\odot}$

LIGO Scientific Collaboration and Virgo Collaboration

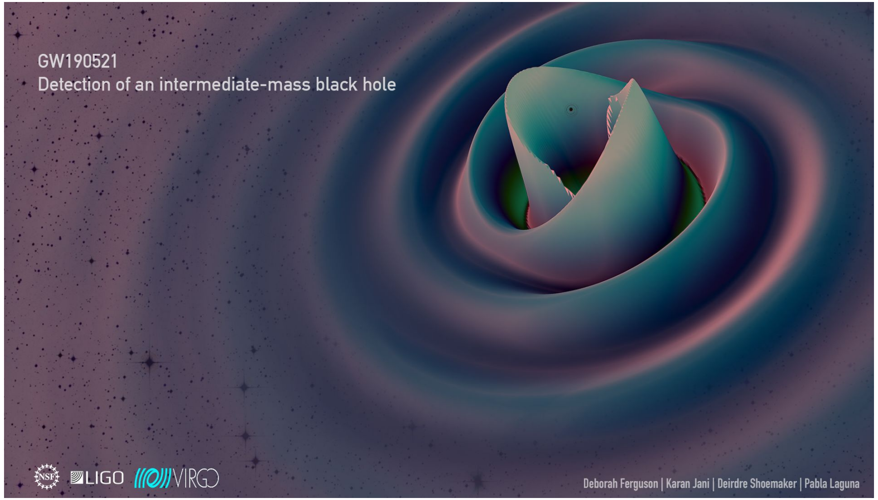

Discovery paper -

Phys. Rev. Lett. 125, 101102 (2020)

https://dcc.ligo.org/LIGO-P2000020/public

(Astro)physical implications -

Astrophys. J. Lett. 900, L13 (2020)

https://dcc.ligo.org/LIGO-P2000021/public

Data release -

https://dcc.ligo.org/LIGO-P2000158/public

Gravitational waves

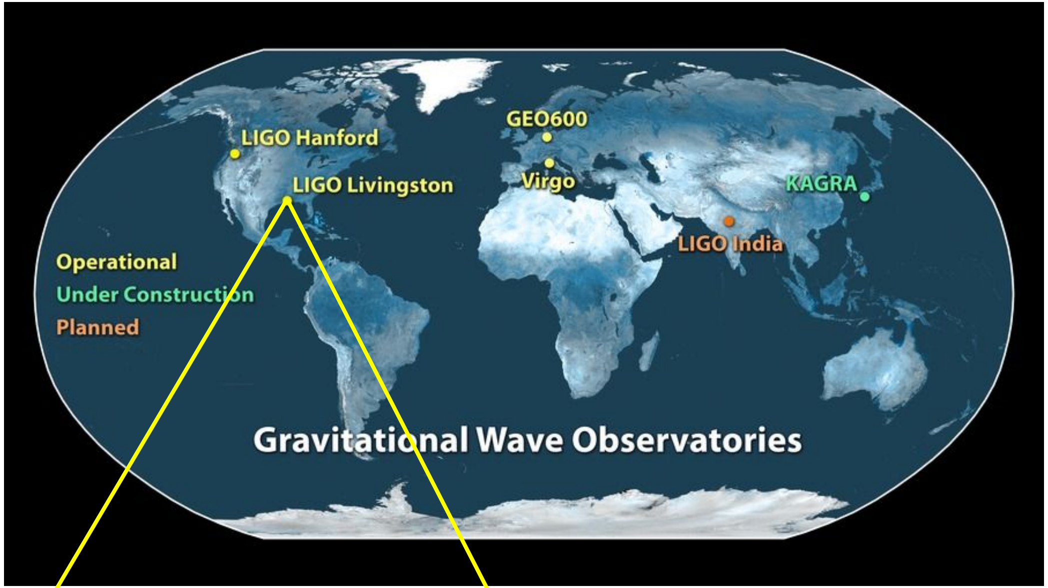

LIGO Livingston

Incoming GWs are measured by the Earth-based detector network

Gravitational waves (GWs) are ripples in spacetime caused by accelerating masses

Some of the best sources of GWs are colliding black holes and neutron stars

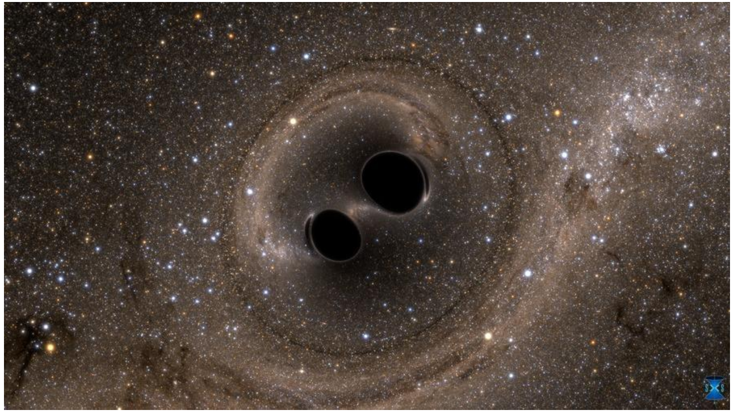

LIGO-Virgo observing runs

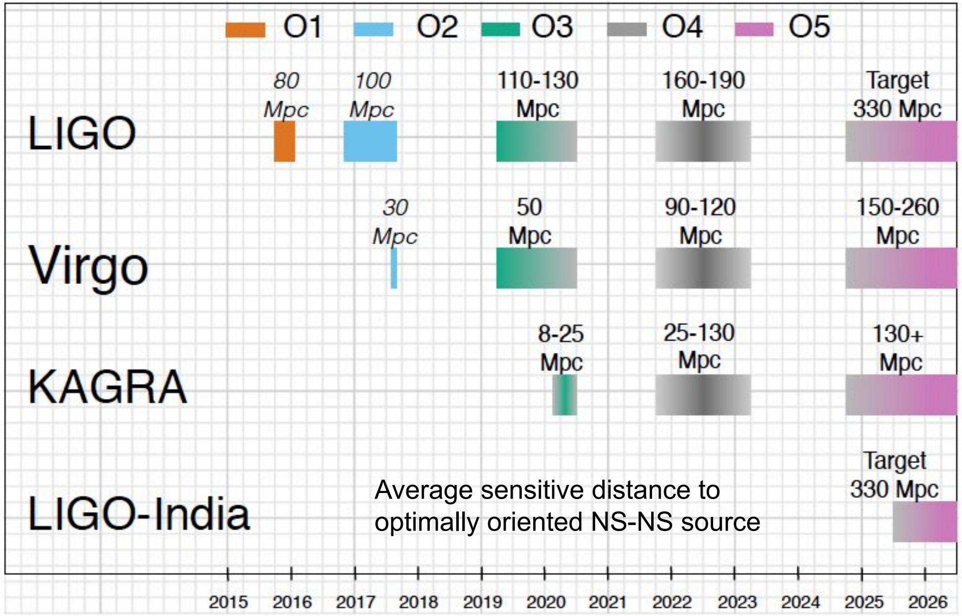

https://dcc.ligo.org/LIGO-P1200087/public

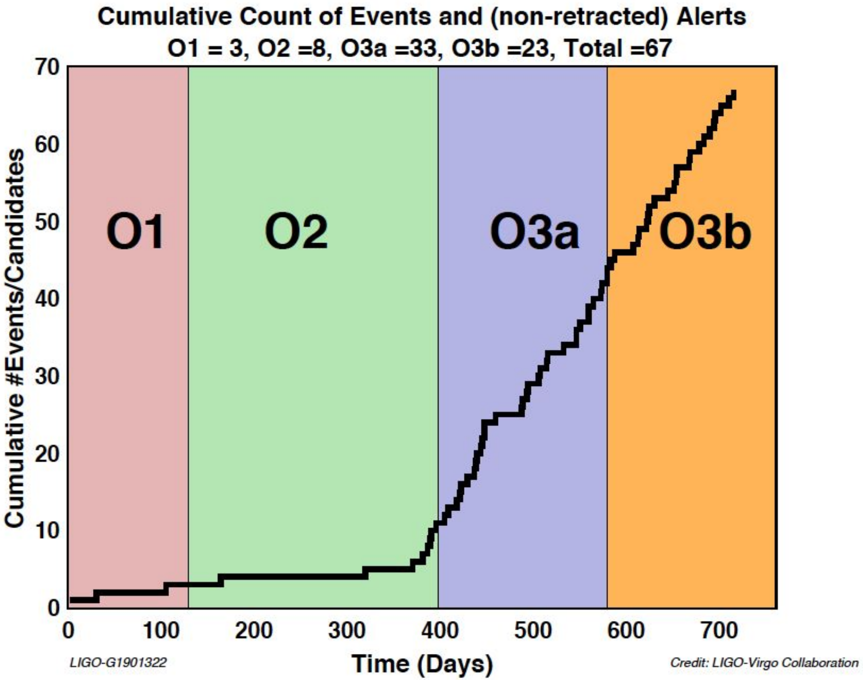

https://dcc.ligo.org/LIGO-G1901322/public

GW190521 in LIGO Hanford, LIGO Livingston, Virgo

GW190521: A Binary Black Hole Merger with a Total Mass of $150 M_\odot$

Properties and astrophysical implications of the $150\,\mathrm{M}_\odot$ binary black hole merger GW190521

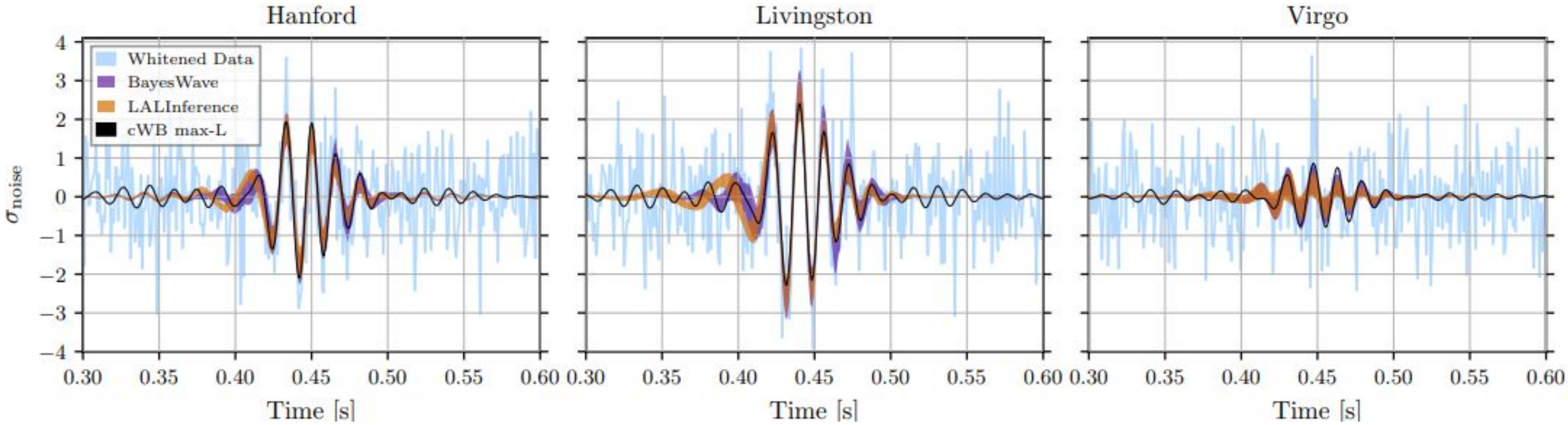

GW190521 signal morphology

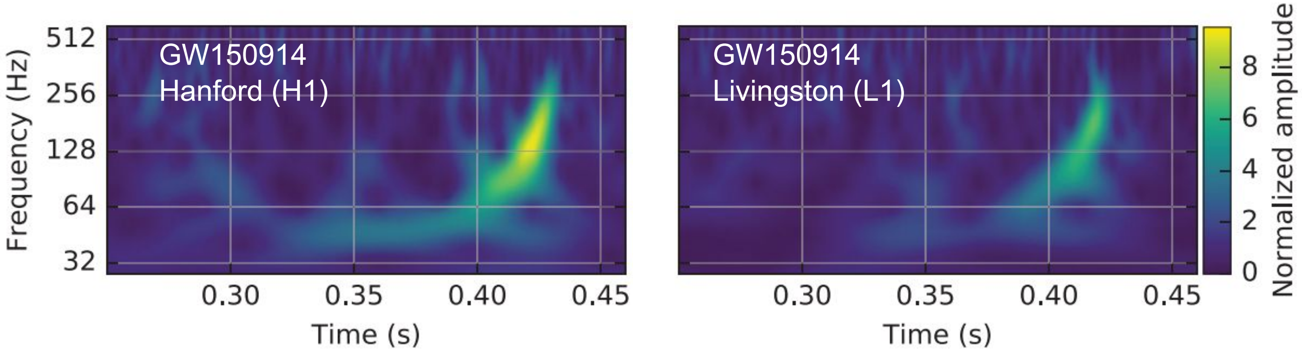

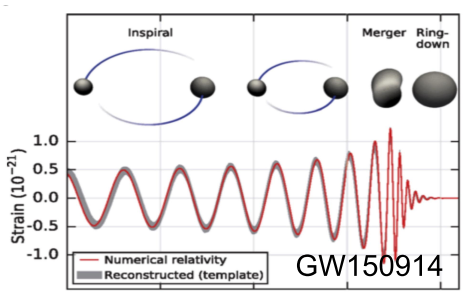

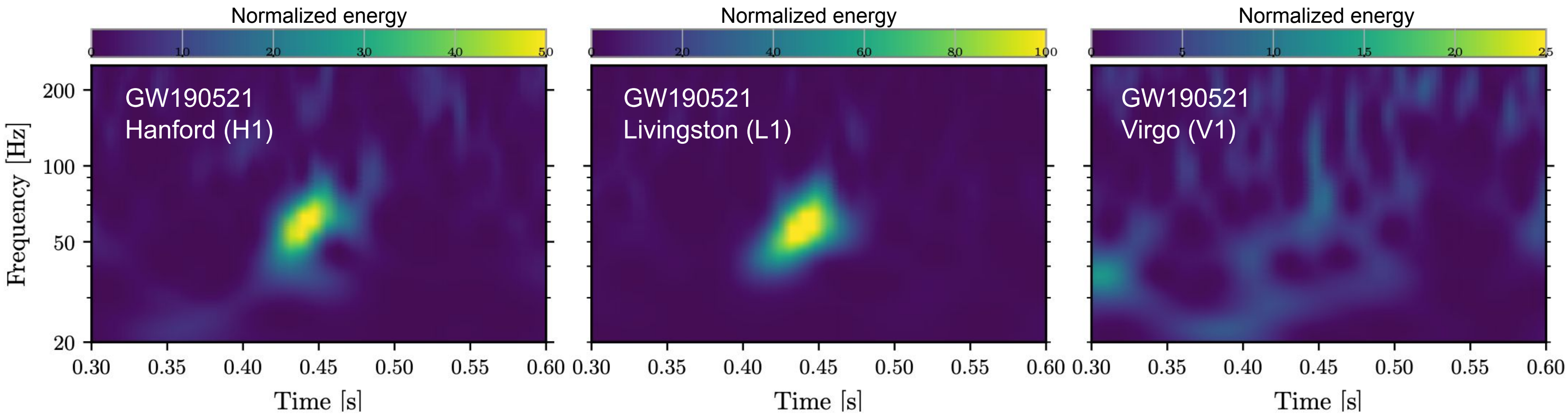

LIGO-Virgo sensitivity to binary black hole mergers

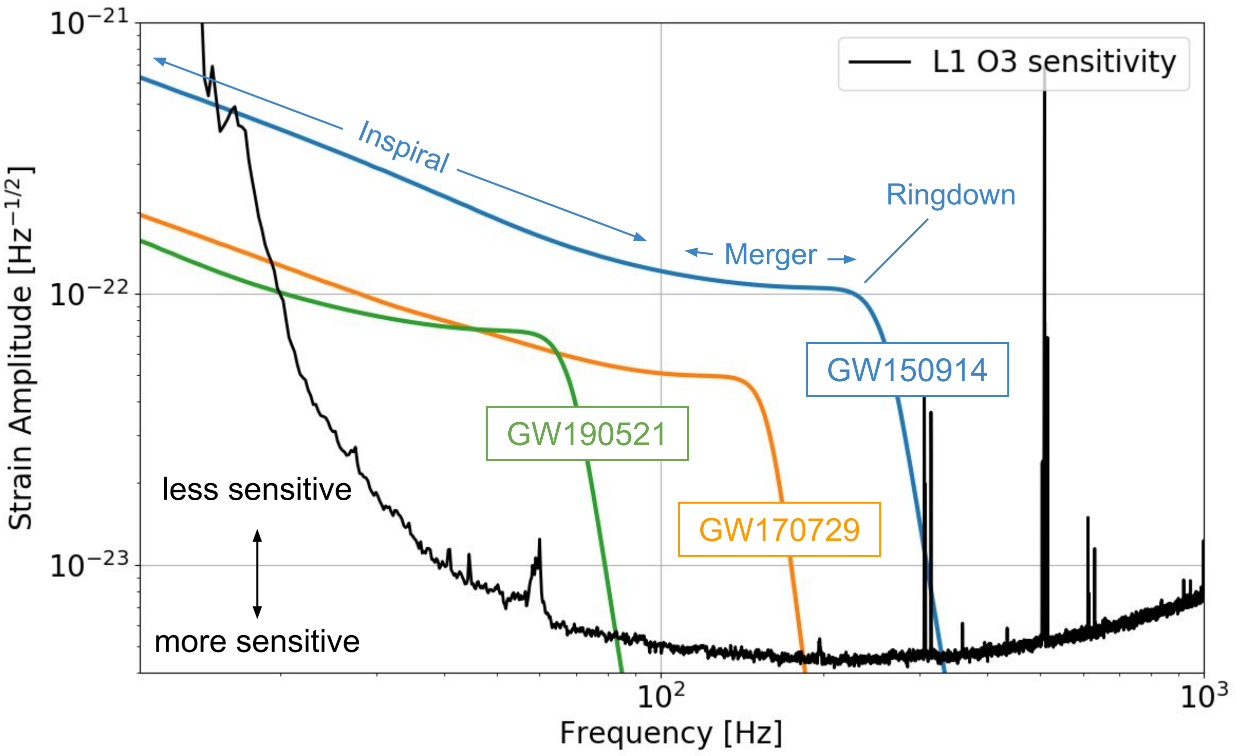

- LIGO-Virgo detectors measure the stretching and squeezing of spacetime caused by a passing GW
- Higher mass binaries correspond to lower frequency GW emission

$$f_{220}^{merger} \sim \frac{c^3}{2\sqrt{2}\pi G M_{tot}(1+z)}$$

- GW signals from highest mass binaries in LIGO-Virgo detectors lack the inspiral (characteristic "chirp")

GW190521 in the context of all LIGO-Virgo detections

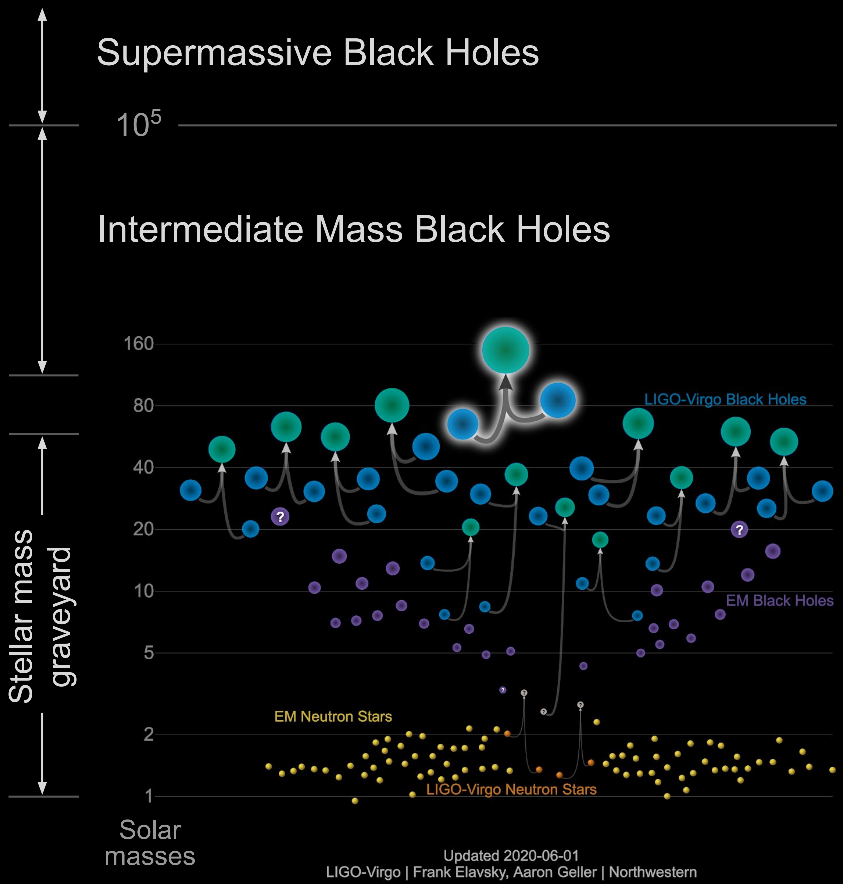

- So far, LIGO-Virgo has reported 12 binary black hole mergers
- The final (remnant) mass of GW190521 is well above 100 solar masses, **marking it as the first intermediate mass black hole (IMBH) detected by LIGO-Virgo**
- **The primary mass lies outside of the stellar mass graveyard (> 65 solar masses)**

LIGO-Virgo component mass

LIGO-Virgo remnant mass

LIGO-Virgo IMBH search sensitivity

LIGO-Virgo sensitive distance in O1-O2

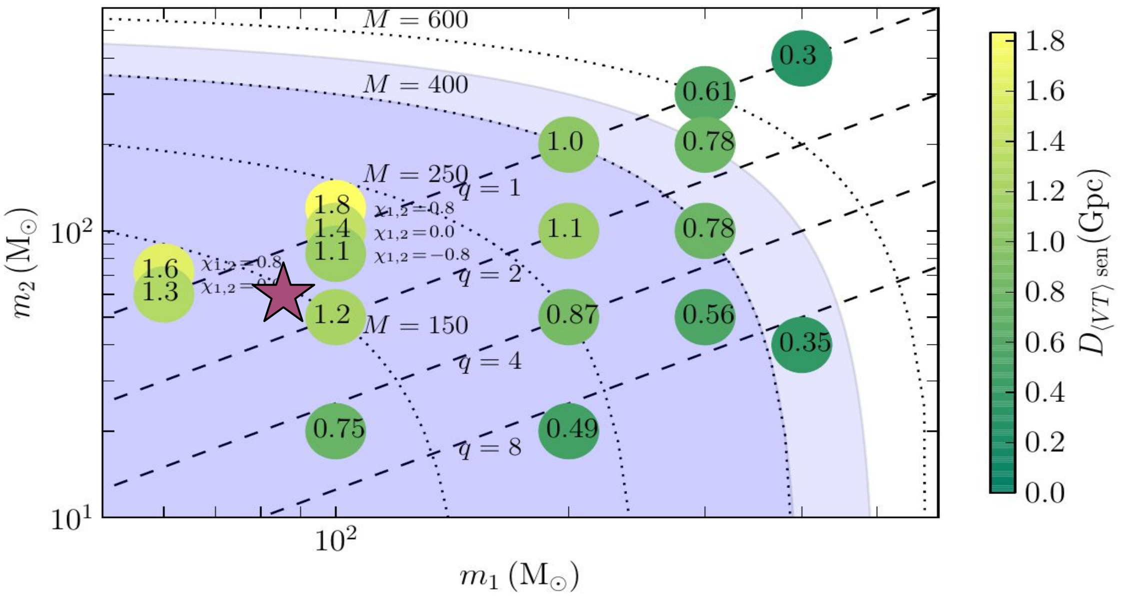

★ GW190521, D_{sen} = 1.7 Gpc (in O3)

Sensitive distance (D_{sen}): a measure of how well we can see a given source type *on average*

IMBH rate upper limit from O1-O2:

$$0.20\,\mathrm{Gpc}^{-3}\,\mathrm{yr}^{-1}$$

Astrophysical merger rate density of GW190521-like events:

(based on one detected event)

$$0.13^{+0.30}_{-0.11}\,\mathrm{Gpc}^{-3}\,\mathrm{yr}^{-1}$$

Searches for GW transients in early O3

Coherent Wave Burst (cWB)

Search for **generic transient signals**

Cross-correlation in the time-frequency (wavelet) domain

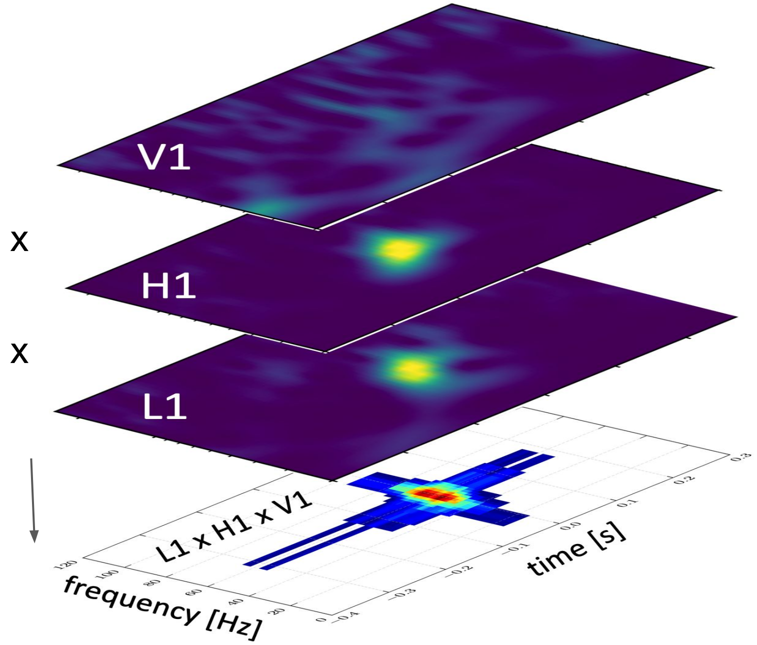

GstLAL, MBTA, PyCBC, SPIIR

Model-based searches for

compact binary coalescences (CBC)

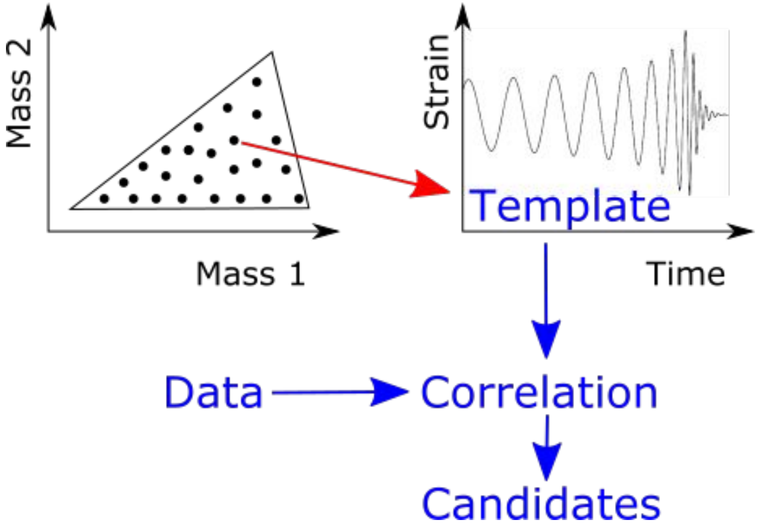

Low-latency discovery of GW190521

Pipeline	Search type	GW190521 results
cWB	Generic transient	Detected with FAR < 1 / 28 yr
GstLAL	CBC	Detected with FAR above alert threshold
MBTA	CBC	Not detected
PyCBC Live	CBC	Detected with FAR ~ 1 / 8 yr
SPIIR	CBC	Detected with FAR above alert threshold

FAR: rate of false alarms ranked higher than the candidate in a given search

6-hr-latency localization using dominant-multipole waveforms w/o precession:

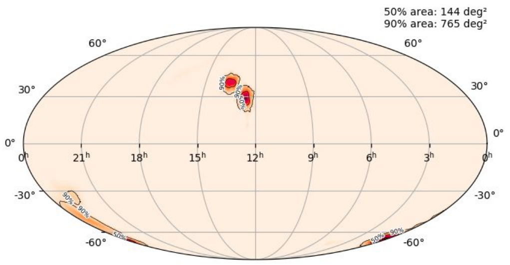

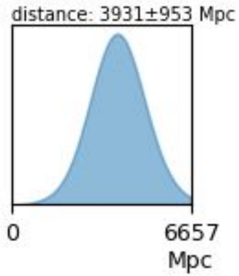

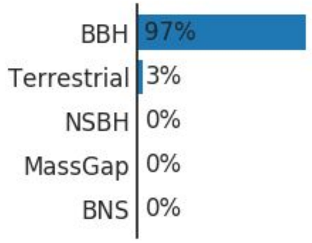

GraceDB page

GW190521 rediscovery with offline (archival) search

- Improve calibration of the data
- Investigate data quality issues, veto contaminated data
- Different analysis
  - Candidate ranking
  - Analyzed interferometers
  - Searched mass range
  - Duration of data used to measure the FAR

Pipeline	Search type	GW190521 results
cWB	Generic transient	Detected with FAR ~ 1 / 4900 yr
GstLAL	CBC	Detected with FAR ~ 1 / 829 yr
PyCBC	CBC	Detected* with FAR ~ 1 / yr

* Masses/spins of GW190521's components at the limit of PyCBC's O3 search range

A special signal

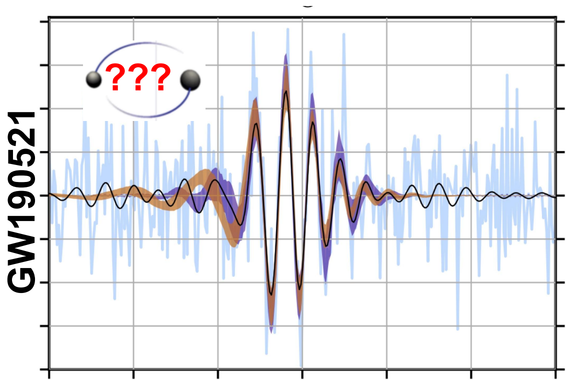

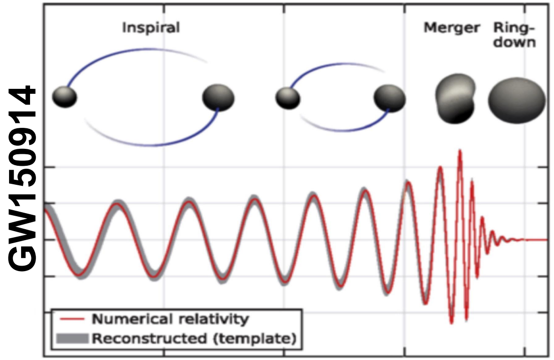

- Very short duration (~0.1 s)
- Low peak frequency (~60 Hz)

→ Massive source

- Standard scenario: quasi-circular BBH merger

  Very short inspiral signal

- Alternative scenarios may be explored:

  Eccentric Binary, Head-on merger

  Cosmic String

Inferring the source properties, assuming quasi-circular BBH

Compare the data to waveform templates for binary black holes:

- Three different template models (NRSurPHM, SEOBPHM, IMRPhenomPHM)
- Numerical simulations
- All include: higher-order multipoles and orbital precession

All models lead to consistent source parameters:

- Discovery paper: results using NRSurPHM.
- Properties & Implications paper: all results.

Masses

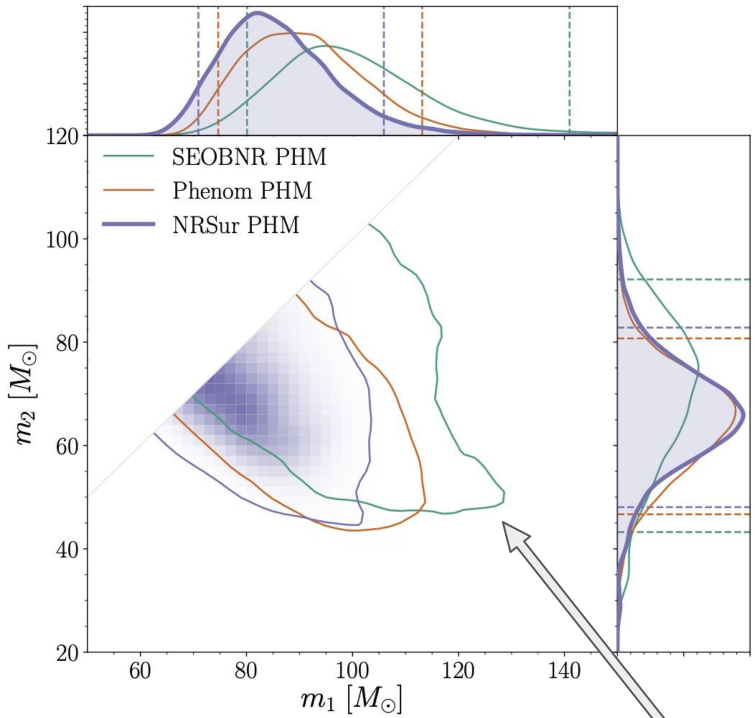

90% credible regions

- Most massive binary ever detected

$$M = 150^{+29}_{-17} M_\odot \qquad m_2/m_1 = 0.79^{+0.19}_{-0.29}$$

- Most massive colliding black holes

$$m_1 = 85^{+21}_{-14} M_\odot \qquad m_2 = 66^{+17}_{-18} M_\odot$$

- Masses within the pair instability supernova gap

$$P(m_1 < 65 M_\odot) = 0.32\%$$

Spins

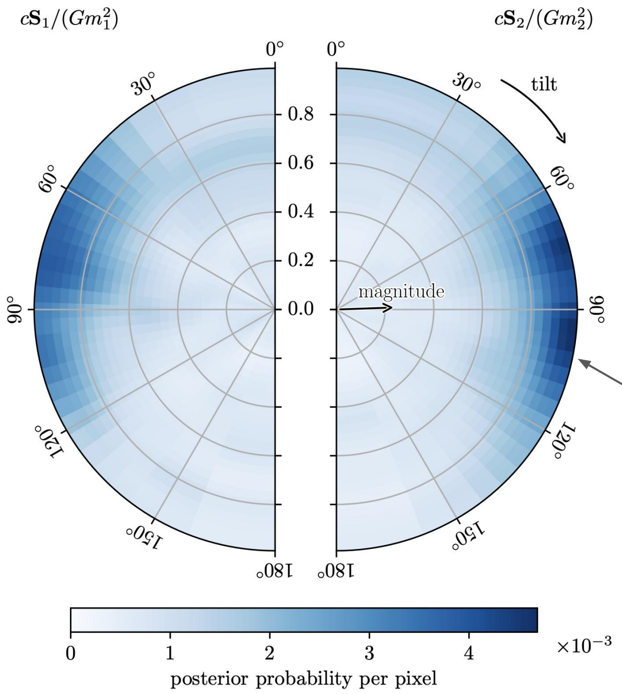

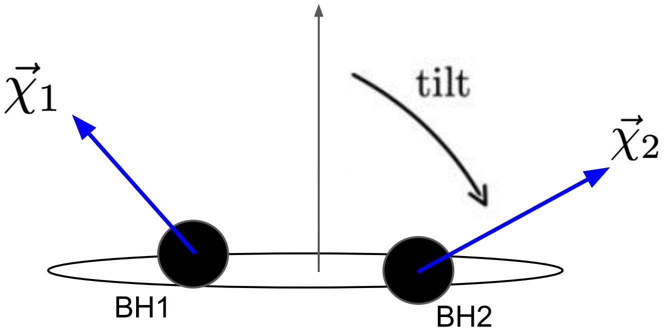

- Spin magnitude $\chi \leq 1$ (cosmic censorship)
- Orientation (or tilt)

Spins

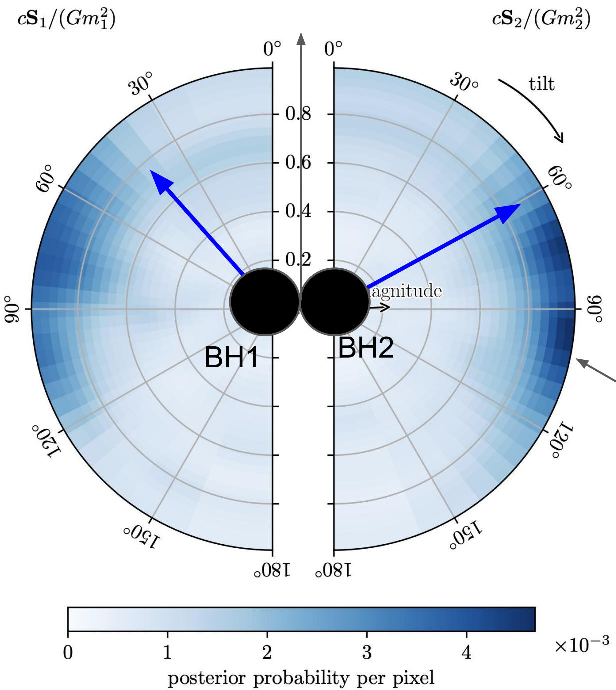

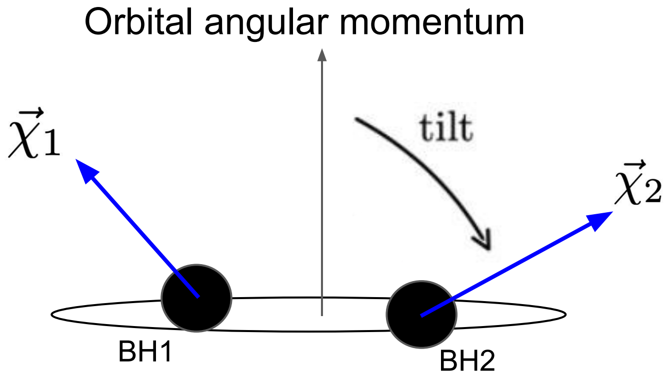

- Spin magnitude $\chi \leq 1$ (cosmic censorship)
- Orientation (or tilt)

Spins

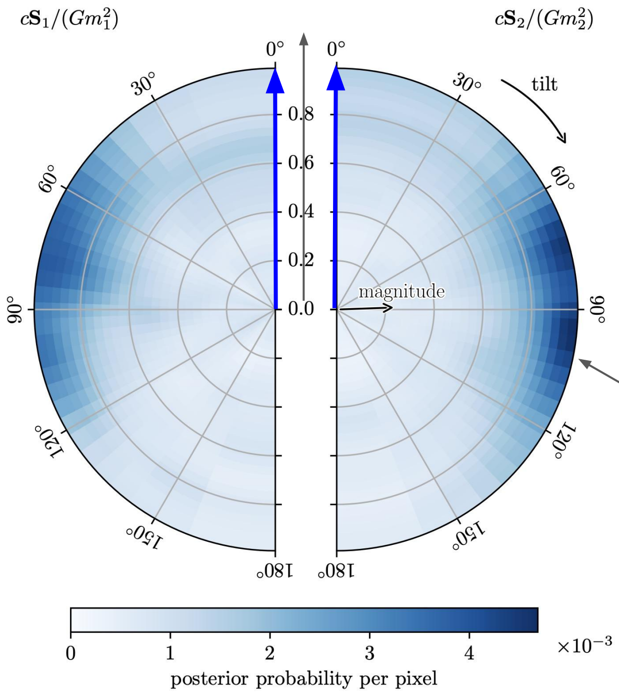

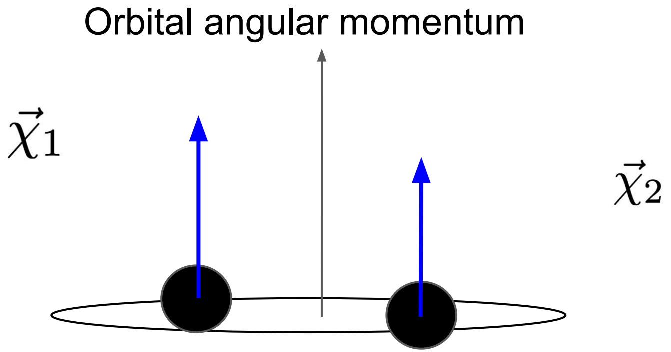

- Spin magnitude $\chi \leq 1$ (cosmic censorship)
- tilt = 0: constant orbital plane

Spins

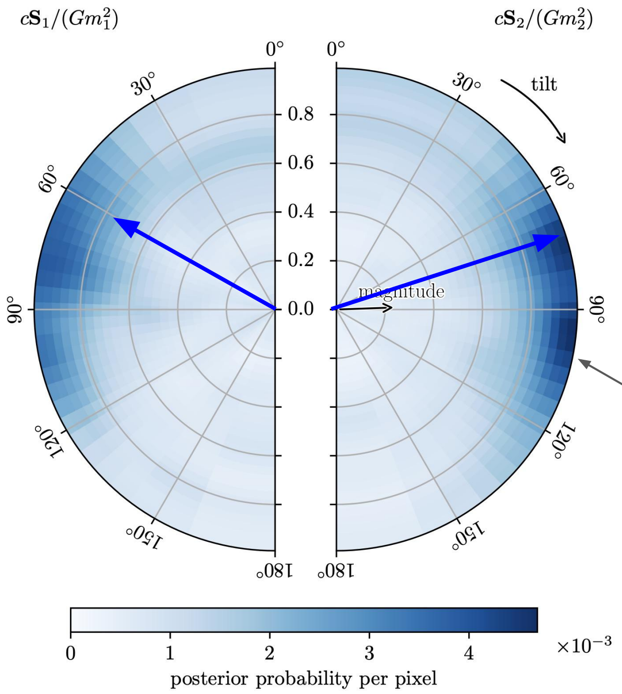

Orbital angular momentum

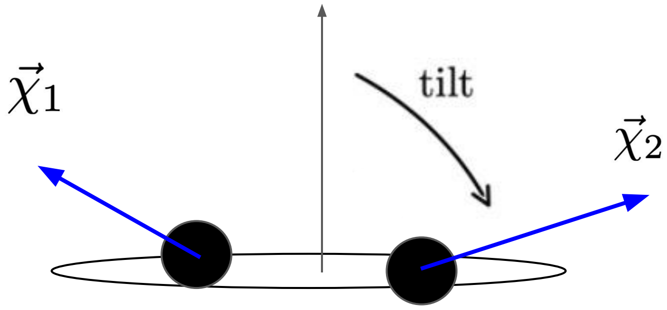

- Spin magnitude $\chi \leq 1$ (cosmic censorship)
- tilt = 0: constant orbital plane
- tilt not 0: orbital precession

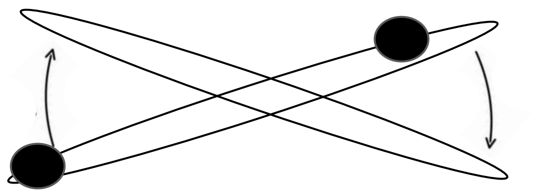

Spins

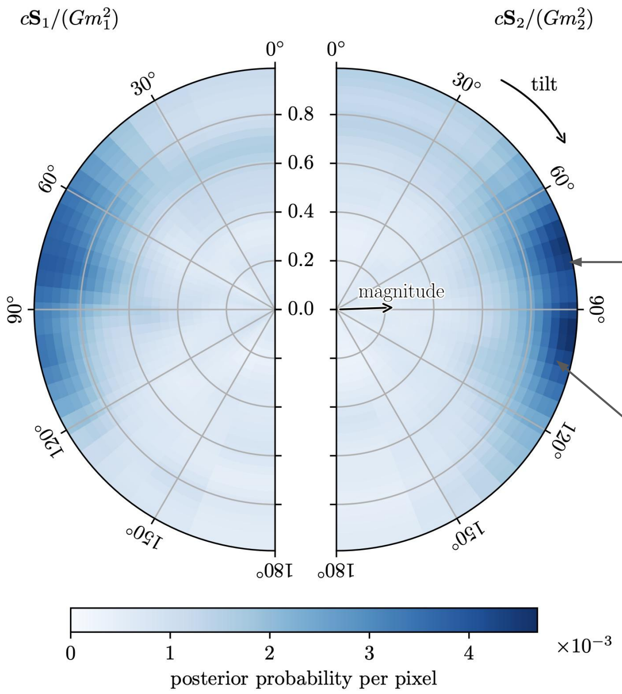

- Spin magnitudes:

$$\chi_1 = 0.69^{+0.27}_{-0.62} \qquad \chi_2 = 0.73^{+0.24}_{-0.64}$$

  - Strong support at $\chi_{1,2} = 1$
  - Also at $\chi_{1,2} = 0$

$$P(\text{Spins vs. No-spins}) = 8.3 : 1$$

- Support for misaligned spins

$$P(\text{Precession vs. No-precession}) = 11.5 : 1$$

Distance and inclination angle

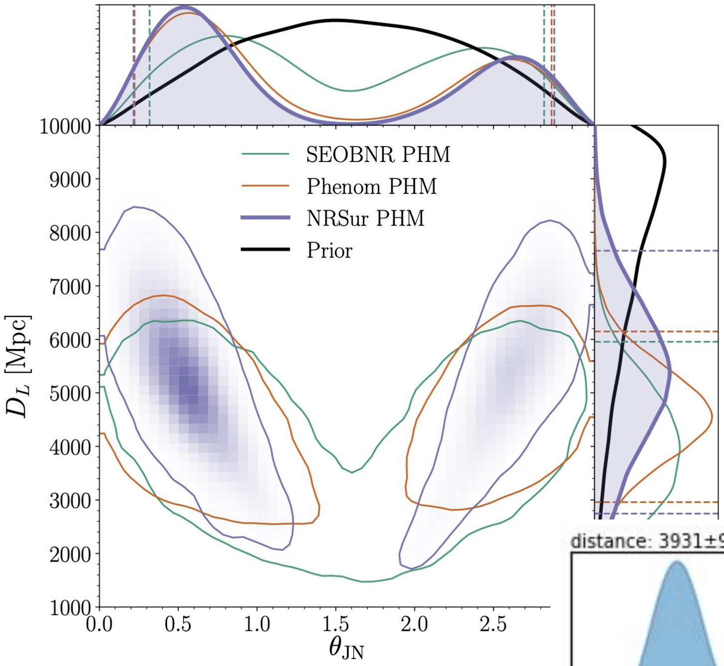

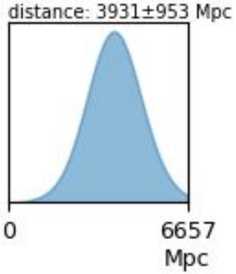

Low latency (6h) estimate: No precession or higher multipoles

- GWs: sum of many emission modes (multipoles)

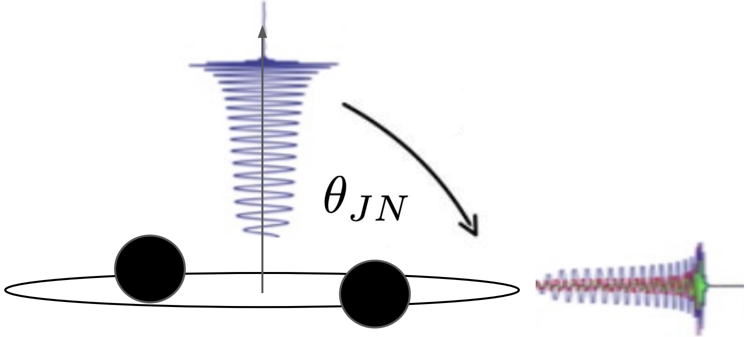

- $\theta_{JN} = 0$: Loud signal, only quadrupole multipole
- $\theta_{JN} \neq 0$: Weaker signal, many multipoles.

$$D_L = 5.3^{+2.4}_{-2.6} Gpc \quad \sin\theta_{JN} < 0.79$$

- No statistical evidence for modes beyond quadrupole

$$P(\text{Higher multipoles vs. Only quadrupole}) = 1 : 2.4$$

Final black hole: mass and spin

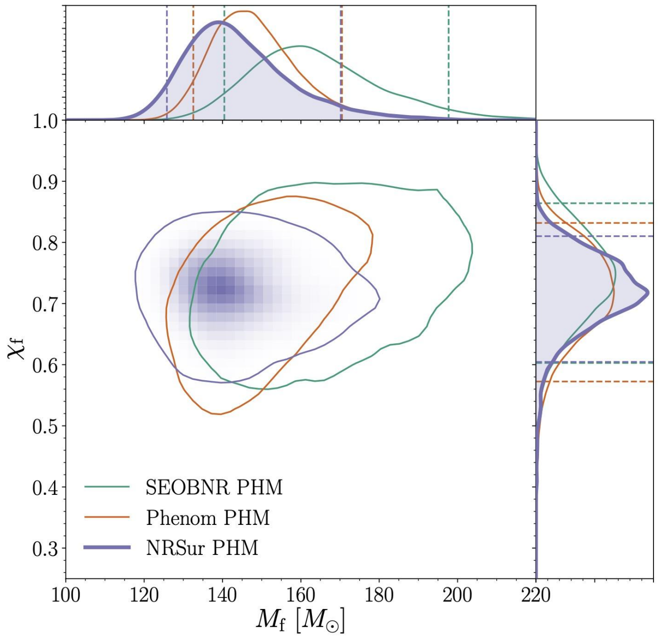

- The binary merger produces a final BH

$$M_f = 142^{+28}_{-16} M_\odot$$

$$E_{GW} \sim 8 M_\odot c^2 \sim 10^{55} erg$$

- No support for $M_f < 100 M_\odot$
  - Most massive BH observed via GWs
  - **First conclusive observation of an intermediate-mass black hole**

- Final spin consistent with the remnant BH of a non-spinning binary

$$\chi_f = 0.72^{+0.09}_{-0.12}$$

Looking at the final black hole: Testing GR

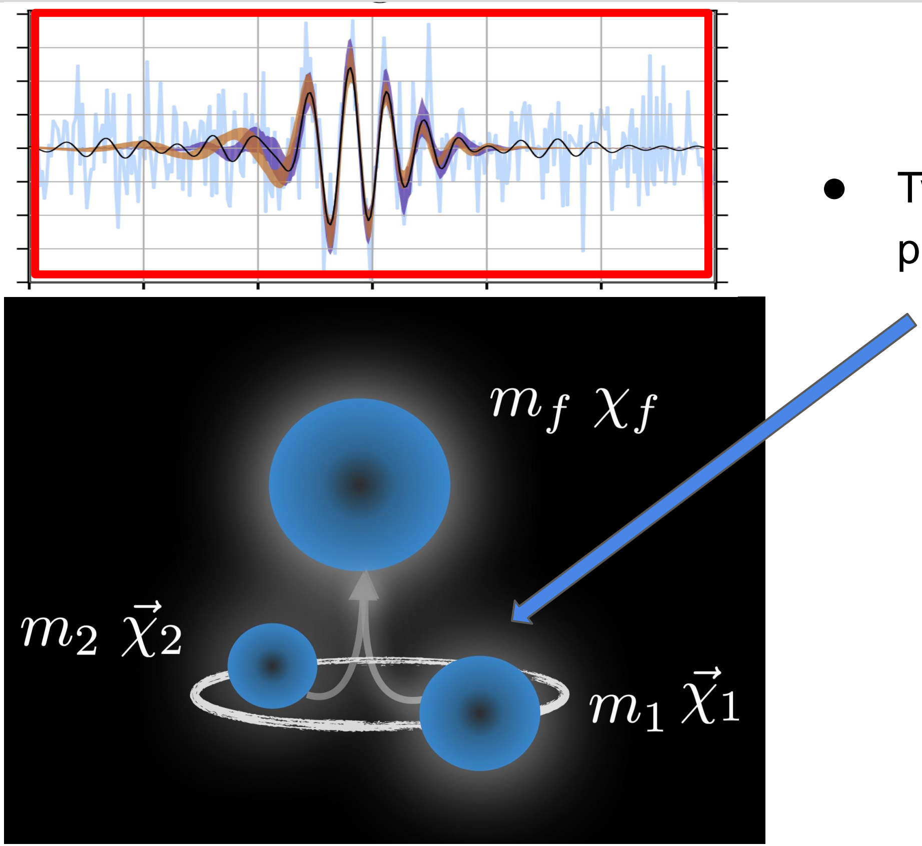

- Two ways to measure the final black hole properties
  - Measure the binary parameters + infer the remnant

Looking at the final black hole: Testing GR

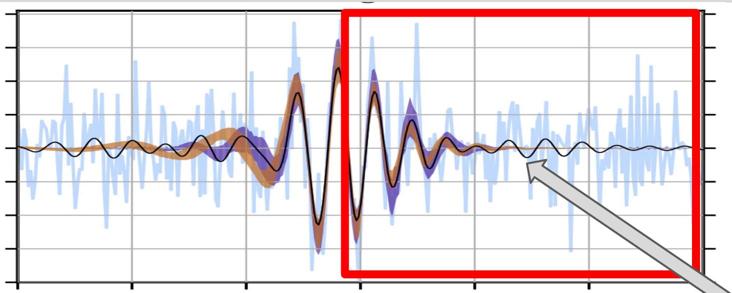

- Two ways to measure the final black hole properties
  - Measure the binary parameters + infer the remnant
  - Directly look at the remnant signal
- Black holes characterised by mass and spin

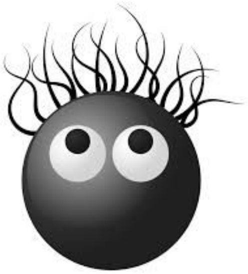

- Material
- Size

- Mass
- Spin

Looking at the final black hole: Testing GR

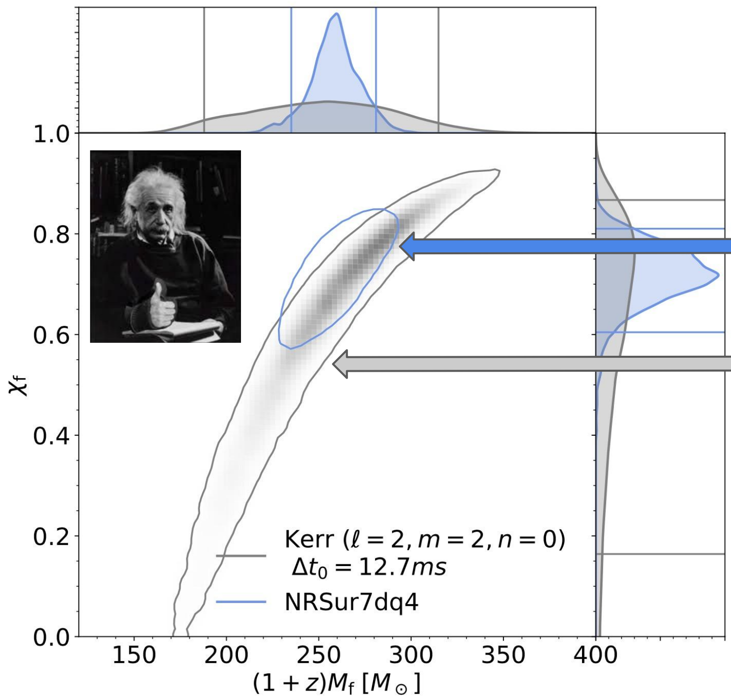

Redshifted mass

- Two ways to measure the final black hole properties
  - Measure the binary parameters + infer the remnant
  - Directly look at the remnant signal
- Black holes characterised by mass and spin
- Comparing both measurements: test of General Relativity
- Both agree

Astrophysical implications

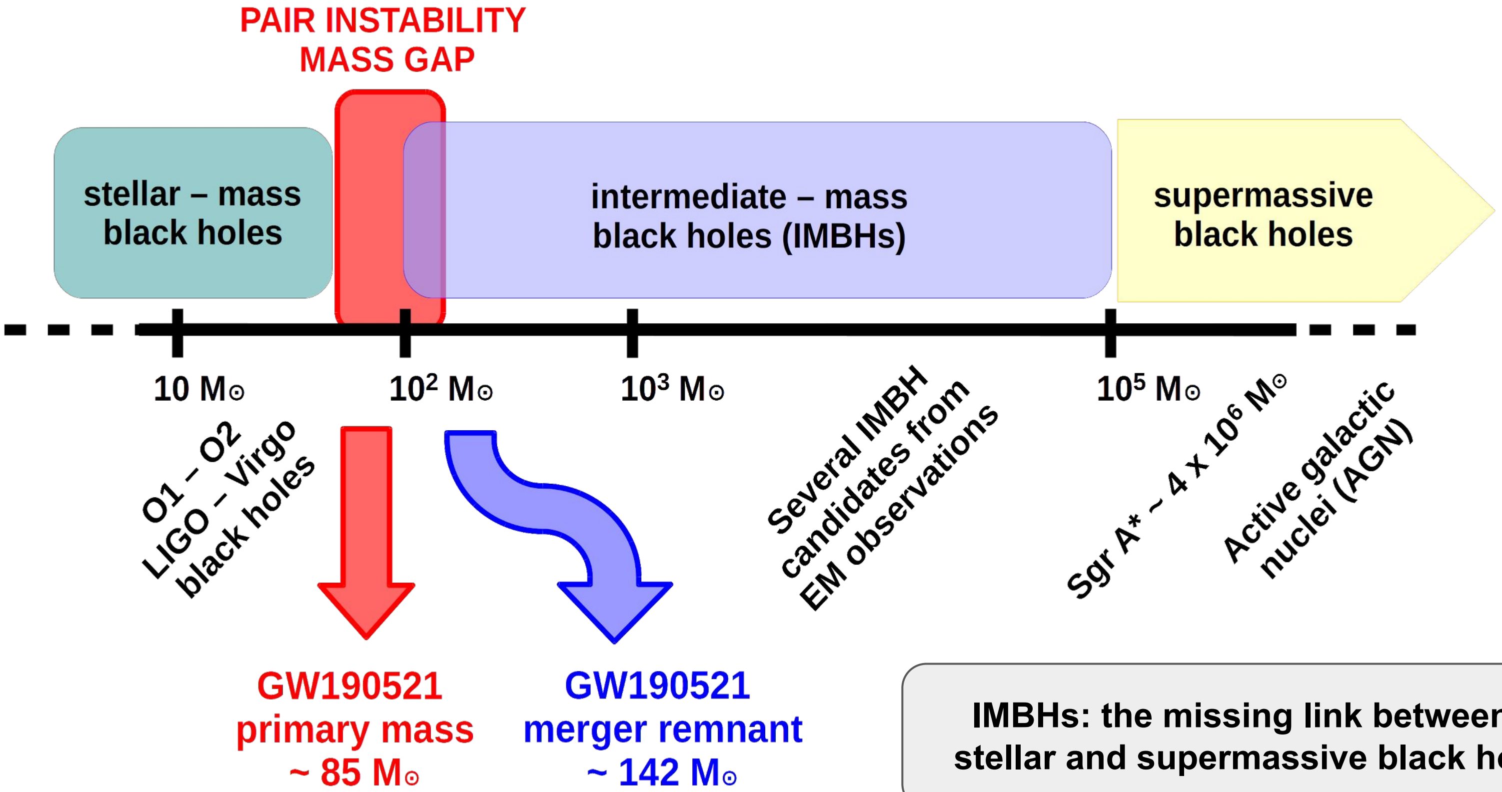

IMBHs: the missing link between stellar and supermassive black holes

Primary component in the pair-instability (PI) mass gap

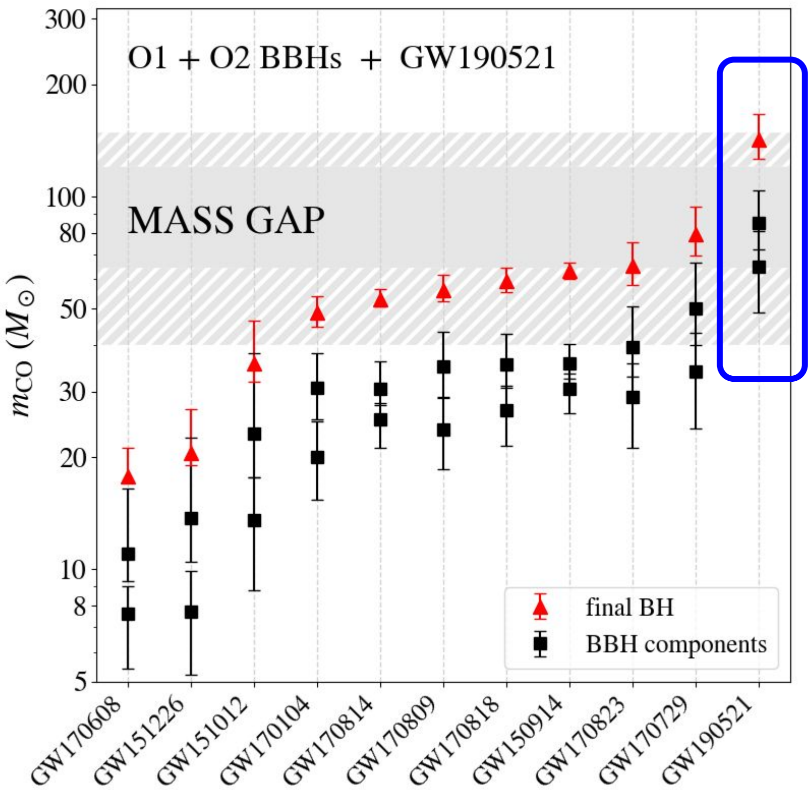

Efficient pair production in massive stars drives (pulsational) pair instability:

opens a gap in ~ 65 - 120 M⊙ range

Large uncertainties on mass gap boundaries:

- Nuclear reaction rates, e.g. $^{12}C(\alpha,\gamma)^{16}O$
- Collapse of hydrogen envelope
- Stellar rotation
- Convection model

CHALLENGE FOR STELLAR EVOLUTION

Dynamical scenarios: Hierarchical mergers

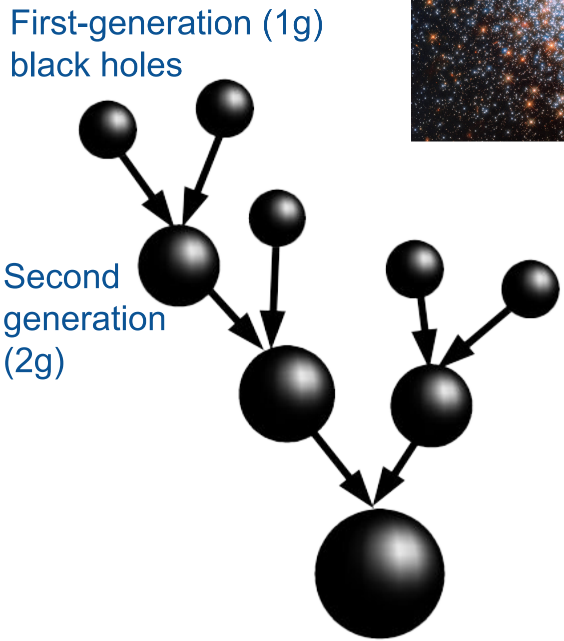

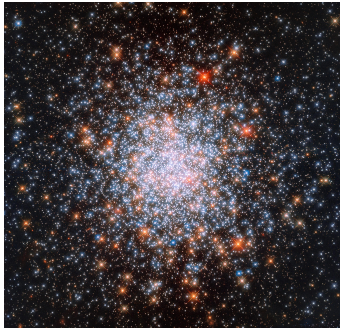

credit: NASA / ESA / Hubble

- Multiple mergers of black holes are possible in dense star clusters and galactic nuclei:
  - mass in the PI gap
  - consistent with $\chi_{eff} \sim 0$ and large χ_p
  - uncertain rates
- **GW170729** final black hole in the PI gap
- Results of hierarchical Bayesian inference on a population model depend strongly on assumed properties of 1g mergers

⟶ no conclusive evidence for GW190521 to be a 2g merger

Dynamical scenarios: Stellar mergers in young star clusters

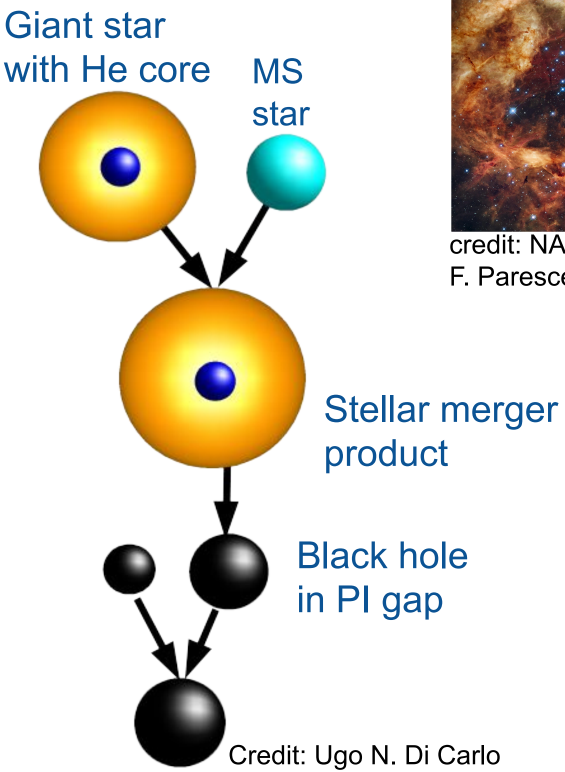

Credit: Ugo N. Di Carlo

credit: NASA, ESA,
F. Paresce, R. O’Connell

- Merger of a massive star with He core and a main sequence (MS) star produces a star with oversized H envelope
- It could collapse to a black hole in the PI gap
- In a dense star cluster, the black hole acquires companions dynamically:
  - primary mass in PI gap
  - consistent with χ_{eff}~ 0 and large χ_p
  - uncertain evolution of stellar collision product
  - rate < 10% of all detectable BBH mergers

Dynamical scenarios: Active galactic nucleus (AGN) disks

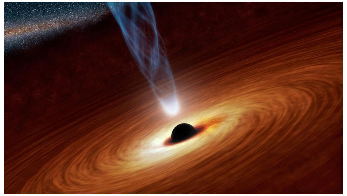

Credit: NASA/JPL-Caltech

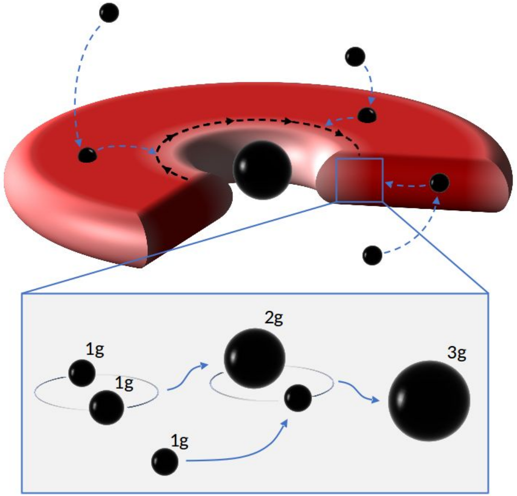

Credit: Imre Bartos

- Gas torques from AGN disks favor black hole pairing and hierarchical mergers
  - primary mass in PI gap
  - large χ_p
  - uncertain rates
  - predicts an EM counterpart

- Candidate optical counterpart in AGN J124942.3+344929 (Graham et al. 2020)

  AGN redshift: z = 0.438

  GW190521 redshift: z = 0.82 (+0.28, -0.34) (90% CI)

Astrophysical implications: Summary

ISOLATED BINARY EVOLUTION:

- Main issue: primary mass in the PI gap
- Uncertainties on stellar evolution leave open the possibility that the lower edge of the mass gap is >65 $M_\odot$

DYNAMICAL SCENARIOS:

- All dynamical scenarios we considered might produce BBHs with mass in the PI gap and large χ_p
- Rates, masses and spins uncertain and model dependent

CHALLENGE FOR DYNAMICAL AND STELLAR EVOLUTION MODELS

Alternative scenarios

HEAD-ON COLLISION or HIGHLY ECCENTRIC MERGER:

- Extremely rare: < 1% of BBH mergers in star clusters

CORE-COLLAPSE SUPERNOVA:

- Inconsistent GW signal morphology
- Non-detection of neutrino signal

PRIMORDIAL BLACK HOLES:

- Exciting scenario for dark matter
- Difficult to constrain

STRONG GRAVITATIONAL LENSING by galaxies or galaxy clusters:

- Low expected lensing rate
- Low optical depth (~10^{-3} - 10^{-4})
- Absence of an identifiable multi-image counterpart

→ no evidence in favor of strong lensing

COSMIC STRINGS:

- Data strongly favor BBH over cosmic string cusp or kink model:

$$\log_{10} \mathrm{BF}\,(\mathrm{BBH}/\mathrm{cusp}) = 29.8$$
$$\log_{10} \mathrm{BF}\,(\mathrm{BBH}/\mathrm{kink}) = 29.7$$

Summary and Conclusions

- GW190521 is **well described by GR waveforms**.
- The GW signal is consistent with a BBH merger source, with total mass of **150 $M_\odot$**.
- The final merged (remnant) black hole is an **Intermediate Mass Black Hole (IMBH)**.
- The more massive of the two BHs in binary is ~ 85 $M_\odot$, **in the Pair Instability Supernova mass gap**.
- It may itself be the result of a previous BBH merger.
- Good agreement between full IMR waveforms from NR, and ringdown-only, as a **test of GR**.
- Forthcoming **Population paper** will address whether GW190521 is consistent with mass distribution of BBHs observed by L-V.

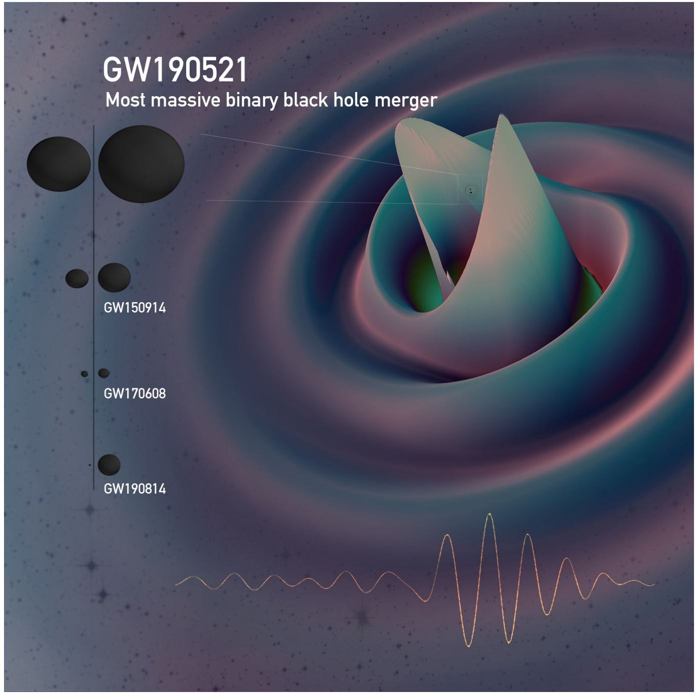

The future is LOUD!

- **LIGO-Virgo-KAGRA** will have a large sample of GW190521-like black holes
- **Next-generation ground- and space-based detectors** (such as LISA) will detect intermediate-mass black holes over a broad range of masses, further deepening our understanding of BBH formation and populations, and providing powerful tests of GR.

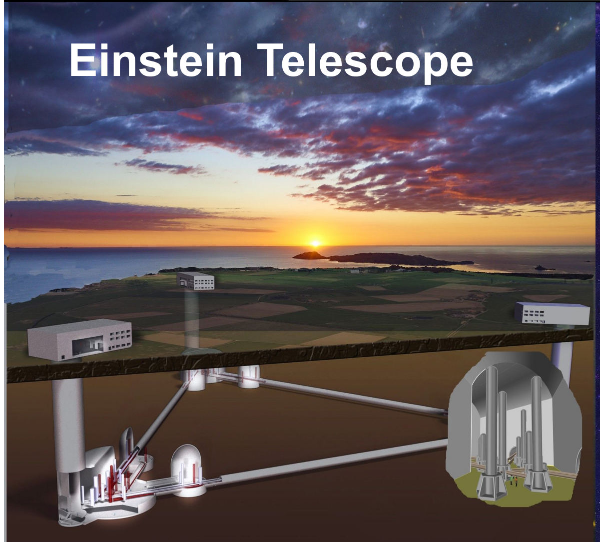

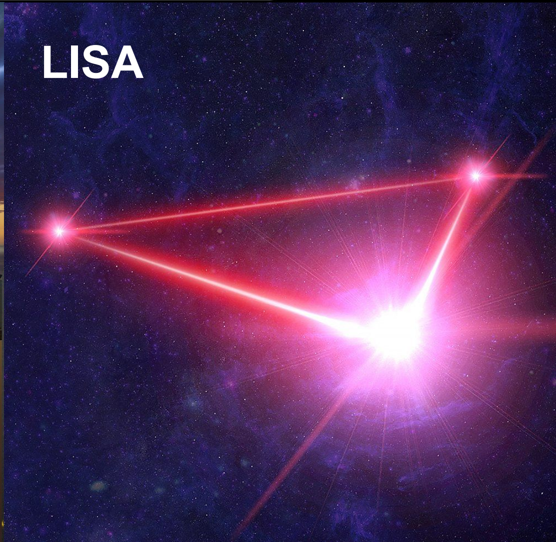

Extra slides

Distance: impact of higher emission multipoles

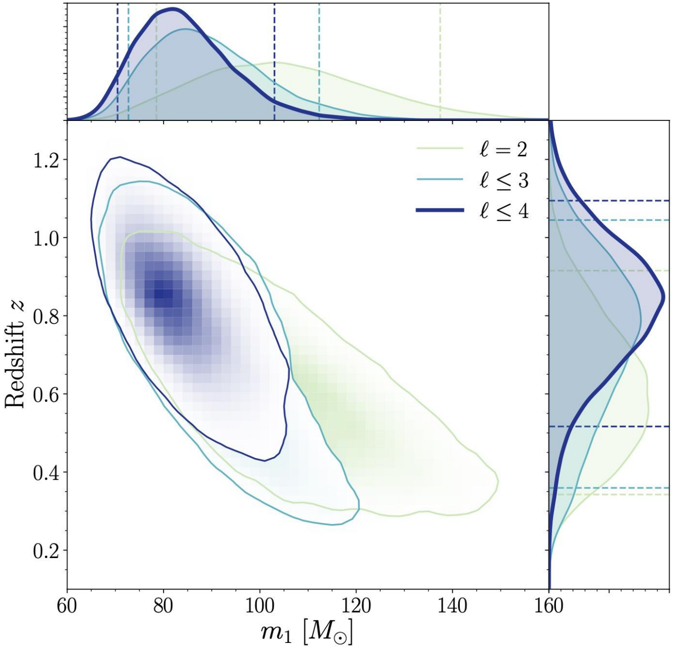

- Higher multipoles break degeneracies
  - Distance and inclination
- Absence of higher modes is informative
  - Inclination must be low
  - The source is further away
- Omission of higher modes:
  - Closer source.
  - Low latency alert:

Spins

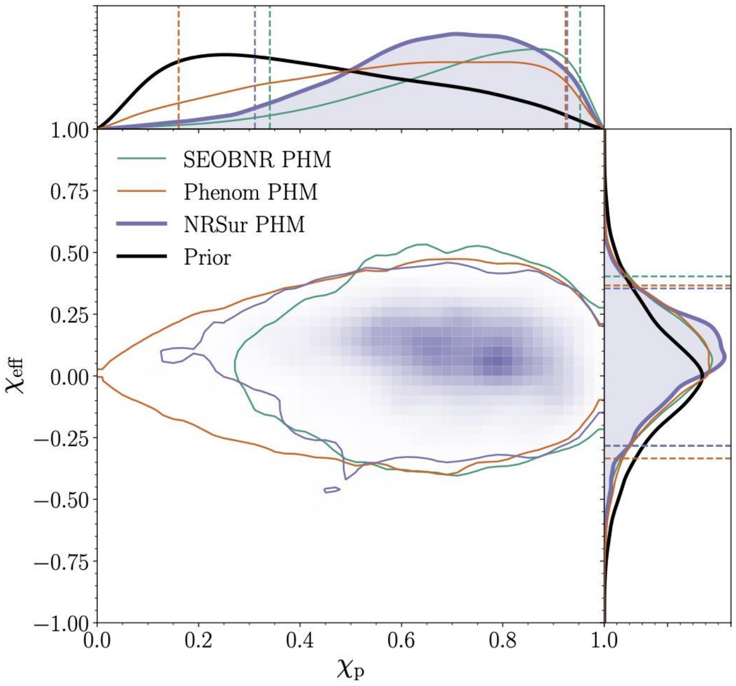

- Spin encoded in two effective parameters

$\chi_{eff} = 0.08^{+0.27}_{-0.36}$ $\chi_p = 0.68^{+0.25}_{-0.37}$

Aligned spins In-plane spins (precession)

- Data barely informative about χ_{eff}
- More information about χ_p

$$Log_{10}\mathcal{B}^{PrecessingSpin}_{Aligned-Spin} = 1.08$$

$$Log_{10}\mathcal{B}^{Spin}_{No-Spin} = 0.92$$

Final black hole: recoil velocity

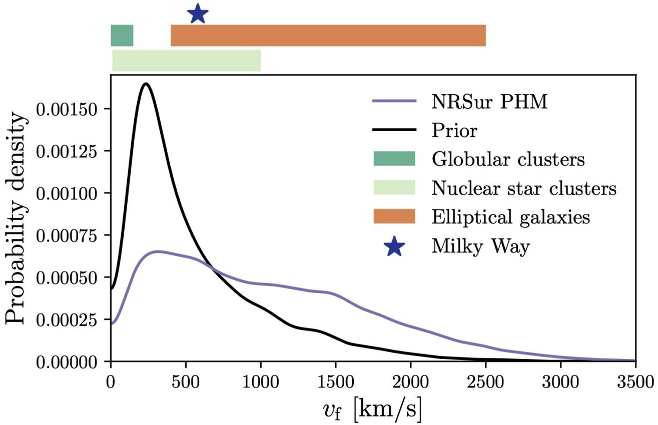

- GW emission is asymmetric
  - Asymmetric emission of linear momentum
  - Final black hole inherits a recoil velocity
- Recoil depends on mass ratio and spins
  - No spins: < 200km/s
  - Aligned-spins: < 500 km/s
  - Precessing spins: up to 5000km/s
- Spins not greatly constrained:
  - Recoil is not well constrained
  - Consistent with retention in XXXX

Bayesian inference on hierarchical mergers

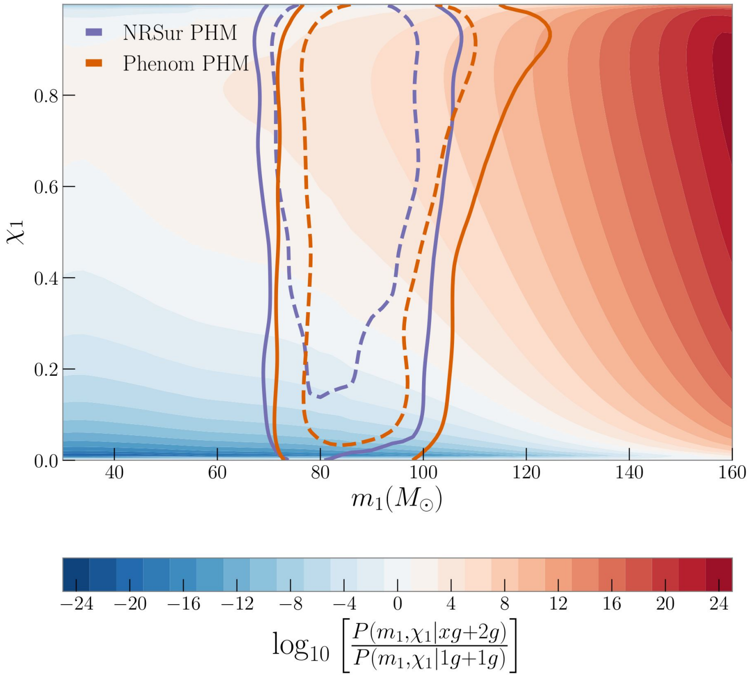

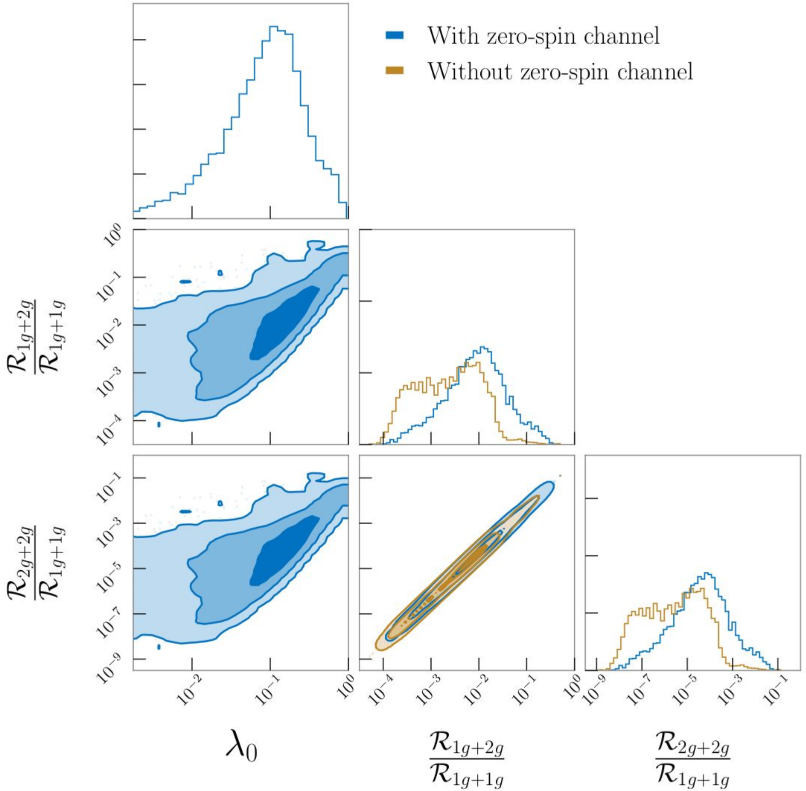

Table

Table 1. Source properties for GW190521: *median values with 90% credible intervals* that include statistical errors.

Waveform Model	NRSur PHM	Phenom PHM	SEOBNR PHM
Primary BH mass m_1 ($M_\odot$)	85^{+21}_{-14}	90^{+23}_{-16}	99^{+42}_{-19}
Secondary BH mass m_2 ($M_\odot$)	66^{+17}_{-18}	65^{+16}_{-18}	71^{+21}_{-28}
Total BBH mass M ($M_\odot$)	150^{+29}_{-17}	154^{+25}_{-16}	170^{+36}_{-23}
Binary chirp mass $\mathcal{M}$ ($M_\odot$)	64^{+13}_{-8}	65^{+11}_{-7}	71^{+15}_{-10}
Mass-ratio $q = m_2/m_1$	$0.79^{+0.19}_{-0.29}$	$0.73^{+0.24}_{-0.29}$	$0.74^{+0.23}_{-0.42}$
Primary BH spin χ_1	$0.69^{+0.27}_{-0.62}$	$0.65^{+0.32}_{-0.57}$	$0.80^{+0.18}_{-0.58}$
Secondary BH spin χ_2	$0.73^{+0.24}_{-0.64}$	$0.53^{+0.42}_{-0.48}$	$0.54^{+0.41}_{-0.48}$
Primary BH spin tilt angle θ_{LS_1} (deg)	81^{+64}_{-53}	80^{+64}_{-49}	81^{+49}_{-45}
Secondary BH spin tilt angle θ_{LS_2} (deg)	85^{+57}_{-55}	88^{+63}_{-58}	93^{+61}_{-60}
Effective inspiral spin parameter χ_{eff}	$0.08^{+0.27}_{-0.36}$	$0.06^{+0.31}_{-0.39}$	$0.06^{+0.34}_{-0.35}$
Effective precession spin parameter χ_{p}	$0.68^{+0.25}_{-0.37}$	$0.60^{+0.33}_{-0.44}$	$0.74^{+0.21}_{-0.40}$
Remnant BH mass M_{f} ($M_\odot$)	142^{+28}_{-16}	147^{+23}_{-15}	162^{+35}_{-22}
Remnant BH spin χ_{f}	$0.72^{+0.09}_{-0.12}$	$0.72^{+0.11}_{-0.15}$	$0.74^{+0.12}_{-0.14}$
Radiated energy E_{rad} ($M_\odot c^2$)	$7.6^{+2.2}_{-1.9}$	$7.2^{+2.7}_{-2.2}$	$7.8^{+2.8}_{-2.3}$
Peak Luminosity ℓ_{peak} (erg s^{-1})	$3.7^{+0.7}_{-0.9} \times 10^{56}$	$3.5^{+0.7}_{-1.1} \times 10^{56}$	$3.5^{+0.8}_{-1.4} \times 10^{56}$
Luminosity distance D_{L} (Gpc)	$5.3^{+2.4}_{-2.6}$	$4.6^{+1.6}_{-1.6}$	$4.0^{+2.0}_{-1.8}$
Source redshift z	$0.82^{+0.28}_{-0.34}$	$0.73^{+0.20}_{-0.22}$	$0.64^{+0.25}_{-0.26}$
Sky localization $\Delta\Omega$ (deg^2)	774	862	1069

Skymap

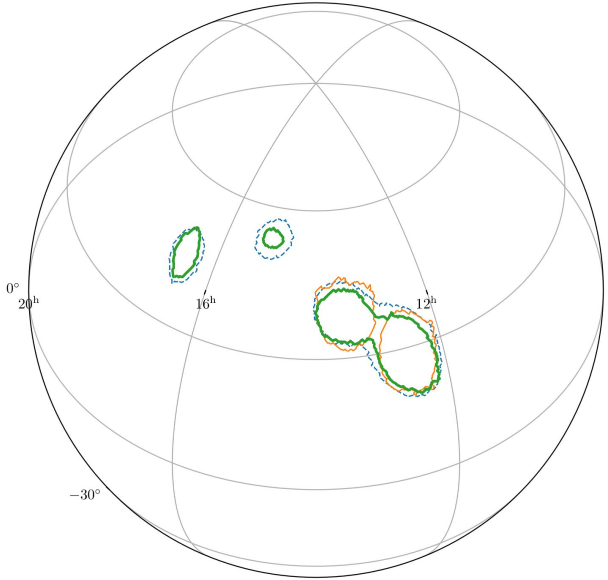

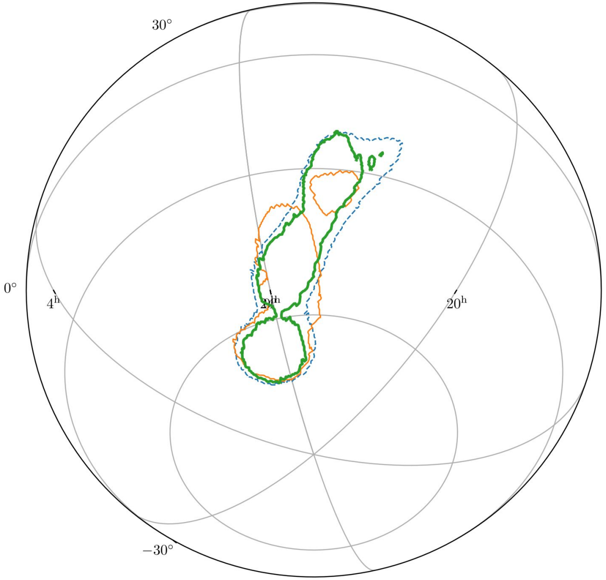

Cosmic Strings

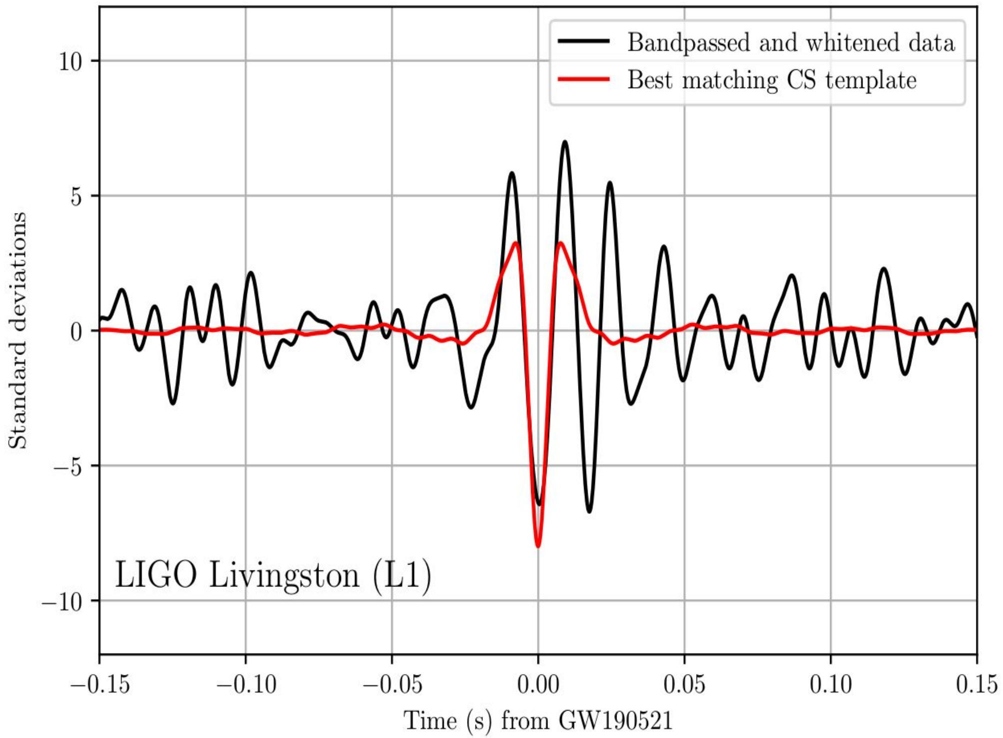

Searches for GW transients in early O3

Weakly-modeled searches for **generic transient signals**

Coherent Wave Burst (cWB)

Relatively insensitive to signal origin and dynamics at the source

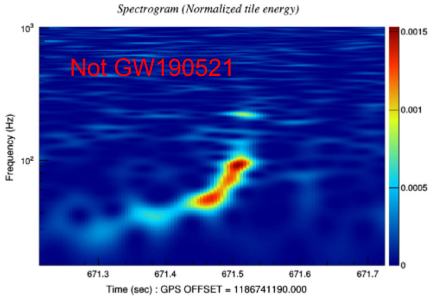

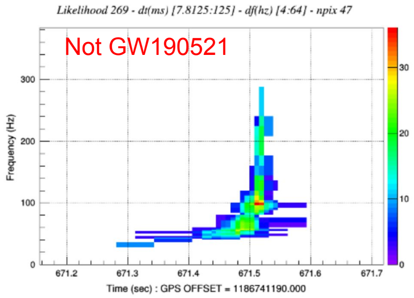

Model-based searches for **compact binary coalescences** with masses from $M_\odot$ to ~$500M_\odot$

GstLAL, MBTA, PyCBC, SPIIR

Balance between physical accuracy, simplicity, sensitivity and computational efficiency

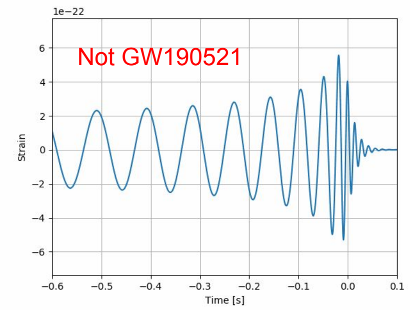

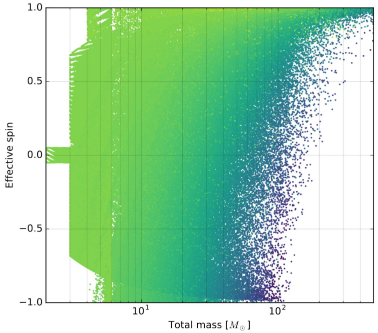

Candidates are assigned a “FAR”

Rate of false alarms ranked higher than the candidate

The FAR is a property of the **search+noise**, not an intrinsic property of the GW signal